Boosting vector leptoquark searches with boosted tops

by

Arvind Bhaskar, Tanumoy Mandal, Subhadip Mitra

in

Physics Review D101

Report No: IIIT/TR/2020/-1

Centre for Computational Natural Sciences and Bioinformatics
International Institute of Information Technology
Hyderabad - 500 032, INDIA
May 2020

Boosting vector leptoquark searches with boosted tops

Arvind Bhaskar,[1,*] Tanumoy Mandal,[2,†] and Subhadip Mitra[1,‡]

[1]*Center for Computational Natural Sciences and Bioinformatics, International Institute of Information Technology, Hyderabad 500 032, India*

[2]*Indian Institute of Science Education and Research Thiruvananthapuram, Vithura, Kerala 695551, India*

(Received 7 April 2020; accepted 21 May 2020; published 15 June 2020)

At the LHC, a TeV-scale leptoquark (LQ) that decays dominantly to a top quark (t) and a light charged lepton ($\ell = e, \mu$) would form a resonance system of *boosted-t*+ high-p_{T}-ℓ. We consider all possible vector LQ models within the Buchmüller-Rückl-Wyler classifications with the desired decay. We propose simple phenomenological Lagrangians that are suitable for bottom-up/experimental studies and, at the same time, can cover the relevant parameter spaces of these models. In this simplified framework, we study the pair and single production channels of vector LQs at the LHC. Interestingly, we find that, like the pair production, the cross sections of some single production processes also depend on the parameter κ that appears in the gluon-vector LQ coupling. We adopt a search strategy of selecting events with at least one boosted hadronic top quark and exactly two high-p_{T} leptons of the same flavor and opposite sign. This combines events from the pair and single production processes and, therefore, can enhance the discovery potential beyond that of the pair-production-only searches. For 5σ discovery we find that vector LQs can be probed up to 2.55 TeV for 100% branching ratio in the $t\ell$ decay mode and $\mathcal{O}(1)$ new couplings at the 14 TeV LHC with 3 ab^{-1} of integrated luminosity.

DOI: 10.1103/PhysRevD.101.115015

I. INTRODUCTION

In the recent past, several experimental collaborations have reported some hints of lepton flavor universality violation in the heavy meson decays. Collectively, these point toward the existence of some physics beyond the Standard Model (SM) as the SM gauge interactions are flavor-blind. Intriguingly, these seem to be quite tenacious and have created a lot of excitement in the particle physics community. Initially, the *BABAR* Collaboration found two significant anomalies in the flavor-changing charged current decays of the B meson via the $b \to c\tau\nu$ transition. They reported the anomalies in terms of excesses in the $R_{D^{(*)}}$ observables defined as the ratios of branching ratios (BRs) to reduce some systematic and hadronic uncertainties [1,2]. Since then, the excesses have survived the later measurements by the LHCb [3–5] and Belle [6–9] collaborations. The statistical average of these two observables obtained in the R_D-R_{D^*} plane by the HFLAV Group puts the anomalies away from the corresponding SM predictions [10–13] by a combined significance of $\sim 3.1\sigma$. The LHCb Collaboration has also observed downward deviations of about 2.5σ [14–18] from the SM predictions [19,20] in the flavor-changing neutral current transition $b \to s\mu\mu$ measured in terms of the $R_{K^{(*)}}$ observables. Similarly, an excess of about $\sim 2\sigma$ was found in another observable, $R_{J/\psi}$ [21]. In addition, a long-standing discrepancy of about $\sim 3.5\sigma$ exists in the muon anomalous magnetic moment measurement [22].

It is known that TeV-scale leptoquarks (LQs) are good candidates to address the flavor anomalies. Moreover, their phenomenology has been explored in various other contexts as well [23–77]. LQs are color-triplet bosons [either scalars (sLQs) or vectors (vLQs)] predicted by many beyond-the-SM theories [78–82]. They have fractional electric charges and carry both lepton and baryon numbers. In general, a LQ can couple to a quark and a lepton of either the same or different generations. The flavor anomalies suggest that LQs couple more strongly to the third-generation fermions than the other two. Cross-generational couplings of LQs could generate flavor-changing neutral currents; those involving the first and second generations are tightly constrained. However, bounds are relatively weaker when a fermion of the third generation is involved.

The search for LQs is an important research program at the LHC. Usually, the LHC searches are done for LQs that

*arvind.bhaskar@research.iiit.ac.in
†tanumoy@iisertvm.ac.in
‡subhadip.mitra@iiit.ac.in

couple to quarks and leptons of the same generation and are labeled accordingly. For example, pair production of a scalar LQ that decays to a top quark and a tau lepton (or a bottom quark and a tau lepton or neutrino), i.e., a third-generation LQ, has been extensively analyzed by both the ATLAS [83,84] and CMS collaborations [85,86]. Altogether, the current bound on the third-generation LQ is roughly about a TeV (this, of course, depends on various assumptions and we refer the reader to the actual papers for details). However, the flavor-motivated LQ models with sizable cross-generational couplings would have exotic signatures and require different search strategies. Of late, the nonstandard decay modes of LQs have started to gain attention; the CMS Collaboration published their first results on the pair production searches of LQs in the $tt\mu\mu$ channel [87]. Based on the 13 TeV data, they performed a prospect study for the pair production of sLQs in the $tt\mu\mu$ channel at the high-luminosity LHC (HL-LHC) [88].

In Ref. [89], we investigated the HL-LHC prospects of sLQs that couple dominantly to the top quark in some detail. There, we focused on charge $1/3$ and $5/3$ sLQs that decay to a top quark and a charged lepton. Even though we considered only third-generation quarks, interestingly, we found that in some scenarios single production can improve their prospects significantly.[1] In this paper, we present a similar follow-up study for vLQs. Here, too, we concentrate on a specific subset of possible vLQs that dominantly couple with a top quark and can decay to a top quark and a light charged lepton (e or μ) with a substantial BR. Since an analysis of the pair production of vLQs that decay to a top quark and a neutrino at the LHC is available in Ref. [90], in this paper we do not analyze this channel again. Instead, we present a set of simplified models that covers all of the possibilities of a vLQ decaying to a top quark and any lepton. These are suitable for experimental analysis. We also demonstrate how they are related to the known models of vLQs [91–94].

Our main motivation for considering this specific type of vLQs is to investigate their collider discovery/exclusion potential by making use of the boosted top signature coming from the LQ decay. They form an exotic resonance system with a boosted top and a high-p_{T} lepton and provide a novel way to search for these models at the LHC. Various flavor anomalies suggest that cross-generational Yukawa-type LQ couplings with tops and leptons might be large. A large coupling makes various single production channels important, especially in the high-mass region. For example, the relevance of the process $gg \to \mathrm{LQ} + t\mu$ was pointed out in Ref. [95]. In our analysis, we adopt the same search strategy as the one we proposed for the sLQs [89]. We identify our signal by selecting at least one boosted hadronic top and exactly two high-p_{T} leptons and use the highest-p_{T} top (if there is more than one top) and one of the selected leptons to reconstruct a heavy system, i.e., the LQ. As we have demonstrated before [89,96–98], such a selection strategy combines pair and single production events and increases the LHC reach. Although pair production is suitable for probing the low-mass region, single production takes over when the LQ becomes heavy. Compared to the sLQs, the pair production cross sections for vLQs are relatively bigger and hence the current mass limits obtained for pair production are generally higher for the vLQs than for the sLQs. In the case of vLQs, the importance of single production becomes visible for relatively higher mass compared to sLQs. We shall see that the discovery prospects of the vLQs at the HL-LHC are significantly improved if the new couplings controlling single production are of order unity.

Before we proceed further, we note that since this paper is a follow-up to Ref. [89], we shall frequently refer to that paper and omit some details that are common while ensuring that our presentation is self-contained. The rest of the paper is organized as follows. In Sec. II we describe the vLQ models and introduce simplified models suitable for experimental analysis. In Sec. III we discuss the LHC phenomenology and illustrate our search strategy, and then we present our estimations in Sec. IV. Finally, we summarize and conclude in Sec. V.

II. VECTOR LEPTOQUARK MODELS

To conserve electromagnetic charge, vLQs that decay to a top-lepton pair would have either electric charge equal to $\pm 1/3$ or $\pm 5/3$ (if the lepton is a charged one), or $2/3$ (if the lepton is a neutrino). This means that among the vLQs listed in Refs. [91–94], the weak singlets U_1 and $\tilde{U}_1$, doublets V_2 and $\tilde{V}_2$, and triplet U_3 would qualify for our study. Below, we display the relevant terms in the interaction Lagrangians, following the notation of Ref. [94]. To avoid proton decay constraints, we ignore the diquark operators.

(i) $\tilde{U}_1 = (\mathbf{3}, \mathbf{1}, 5/3)$: The electric charge of $\tilde{U}_1$ is $5/3$. Hence, it couples exclusively with the right-handed leptons:

$$\mathcal{L} \supset \tilde{x}^{RR}_{1\,ij} \bar{u}^i_R \gamma^\mu \tilde{U}_{1,\mu} \ell^j_R + \mathrm{H.c.}, \tag{1}$$

where u_R and ℓ_R are a SM right-handed up-type quark and a charged lepton, respectively, and $i, j = \{1, 2, 3\}$ are the generation indices. The color indices are suppressed. For our purpose, we consider only those terms that would connect a vLQ to a third-generation quark and ignore the rest,

$$\mathcal{L} \supset \tilde{x}^{RR}_{1\,3j} \bar{t}_R (\gamma \cdot \tilde{U}_1) \ell^j_R + \mathrm{H.c.} \tag{2}$$

[1]This is interesting because, when a LQ (or any other particle) mostly couples to the third-generation quarks, we generally expect their single production to be ignorable as the bottom (top) quark density in the proton is too small (nonexistent) to play any significant role at the LHC.

(ii) $U_1 = (\mathbf{3}, \mathbf{1}, 2/3)$: The necessary interaction terms for the charge-$2/3$ U_1 can be written as

$$\mathcal{L} \supset x^{LL}_{1\,ij} \bar{Q}^i_L \gamma^\mu U_{1,\mu} L^j_L + x^{RR}_{1\,ij} \bar{d}^i_R \gamma^\mu U_{1,\mu} \ell^j_R + \text{H.c.}, \tag{3}$$

where Q_L, L_L, and d_R are the SM left-handed quark doublet, lepton doublet, and a down-type right-handed quark, respectively. The $i = 3$ terms can be written explicitly as

$$\begin{aligned}\mathcal{L} \supset\ & x^{LL}_{1\,3j} \{\bar{t}_L (\gamma \cdot U_1) \nu^j_L + \bar{b}_L (\gamma \cdot U_1) \ell^j_L\} \\ & + x^{RR}_{1\,3j} \bar{b}_R (\gamma \cdot U_1) \ell^j_R + \text{H.c.}\end{aligned} \tag{4}$$

(iii) $V_2 = (\bar{\mathbf{3}}, \mathbf{2}, 5/6)$: For V_2, the Lagrangian is as follows:

$$\begin{aligned}\mathcal{L} \supset\ & x^{RL}_{2\,ij} \bar{d}^{Ci}_R \gamma^\mu V^a_{2,\mu} \epsilon^{ab} L^{jb}_L \\ & + x^{LR}_{2\,ij} \bar{Q}^{Ci,a}_L \gamma^\mu \epsilon^{ab} V^b_{2,\mu} \ell^j_R + \text{H.c.}\end{aligned} \tag{5}$$

The superscript C denotes charge conjugation. Expanding the Lagrangian, we get

$$\begin{aligned}\mathcal{L} \supset\ & -(x^{RL}_2 \mathbf{U})_{ij} \bar{d}^{Ci}_R \gamma^\mu V^{1/3}_{2,\mu} \nu^j_L + x^{RL}_{2\,ij} \bar{d}^{Ci}_R \gamma^\mu V^{4/3}_{2,\mu} \ell^j_L \\ & + (\mathbf{V}^T x^{LR}_2)_{ij} \bar{u}^{Ci}_L \gamma^\mu V^{1/3}_{2,\mu} \ell^j_R \\ & - x^{LR}_{2\,ij} \bar{d}^{Ci}_L \gamma^\mu V^{4/3}_{2,\mu} \ell^j_R + \text{H.c.},\end{aligned} \tag{6}$$

where $\mathbf{U}$ and $\mathbf{V}$ represent the Pontecorvo-Maki-Nakagawa-Sakata neutrino mixing matrix and the Cabibbo-Kobayashi-Maskawa (CKM) quark mixing matrix, respectively. We assume $\mathbf{U}$ to be unity, as the LHC is blind to the flavor of the neutrinos. Similarly, since the small off-diagonal terms of the CKM matrix play a negligible role at the LHC, we assume a diagonal CKM matrix for simplicity. Hence, the terms relevant for our analysis are

$$\begin{aligned}\mathcal{L} \supset\ & -x^{RL}_{2\,3j} \bar{b}^C_R \{(\gamma \cdot V^{1/3}_2) \nu^j_L - (\gamma \cdot V^{4/3}_2) \ell^j_L\} \\ & + x^{LR}_{2\,3j} \{\bar{t}^C_L (\gamma \cdot V^{1/3}_2) - \bar{b}^C_L (\gamma \cdot V^{4/3}_2)\} \ell^j_R + \text{H.c.}\end{aligned} \tag{7}$$

(iv) $\tilde{V}_2 = (\bar{\mathbf{3}}, \mathbf{2}, -1/6)$: For $\tilde{V}_2$, the Lagrangian becomes

$$\mathcal{L} \supset \tilde{x}^{RL}_{2\,ij} \bar{u}^{C\,i}_R \gamma^\mu \tilde{V}^b_{2,\mu} \epsilon^{ab} L^{j,a}_L + \text{H.c.} \tag{8}$$

Expanding it, we get

$$\begin{aligned}\mathcal{L} \supset\ & -\tilde{x}^{RL}_{2\,ij} \bar{u}^{C\,i}_R \gamma^\mu \tilde{V}^{1/3}_{2,\mu} \ell^j_L + (\tilde{x}^{RL}_2 U)_{ij} \bar{u}^{C\,i}_R \gamma^\mu \tilde{V}^{-2/3}_{2,\mu} \nu^j_L \\ & + \text{H.c.}\end{aligned} \tag{9}$$

The terms with the third-generation quarks are

$$\mathcal{L} \supset \tilde{x}^{RL}_{2\,3j} \bar{t}^C_R \{-(\gamma \cdot \tilde{V}^{1/3}_2) \ell^j_L + (\gamma \cdot \tilde{V}^{-2/3}_2) \nu^j_L\} + \text{H.c.} \tag{10}$$

(v) $U_3 = (\mathbf{3}, \mathbf{3}, 2/3)$: The necessary interaction terms for the triplet U_3 are

$$\mathcal{L} \supset x^{L\,L}_{3\,ij} \bar{Q}^{i,a}_L \gamma^\mu (\tau^k U^k_{3,\mu})^{ab} L^{j,b}_L + \text{H.c.}, \tag{11}$$

where τ^k denotes the Pauli matrices. This can be expanded as

$$\begin{aligned}\mathcal{L} \supset\ & -x^{LL}_{3\,ij} \bar{d}^i_L \gamma^\mu U^{2/3}_\mu \ell^j_L + (\mathbf{V} x^{LL}_3 \mathbf{U})_{ij} \bar{u}^i_L \gamma^\mu U^{2/3}_\mu \nu^j_L \\ & + \sqrt{2} (x^{LL}_3 \mathbf{U})_{ij} \bar{d}^i_L \gamma^\mu U^{-1/3}_\mu \nu^j_L \\ & + \sqrt{2} (\mathbf{V} x^{LL}_3)_{ij} \bar{u}^i_L \gamma^\mu U^{5/3}_\mu \ell^j_L + \text{H.c.}\end{aligned} \tag{12}$$

The terms for the third-generation quarks can be written explicitly as

$$\begin{aligned}\mathcal{L} \supset\ & x^{LL}_{3\,3j} \{-\bar{b}_L (\gamma \cdot U^{2/3}_3) \ell^j_L + \bar{t}_L (\gamma \cdot U^{2/3}_3) \nu^j_L \\ & + \sqrt{2} \bar{b}_L (\gamma \cdot U^{-1/3}_3) \nu^j_L + \sqrt{2} \bar{t}_L (\gamma \cdot U^{5/3}_3) \ell^j_L\} \\ & + \text{H.c.}\end{aligned} \tag{13}$$

A. Simplified model and benchmark scenarios

The above models can be simplified into the following phenomenological Lagrangians:

$$\begin{aligned}\mathcal{L} \supset\ & \Lambda_\ell \{\sqrt{\eta_R} \bar{t}^C_L (\gamma \cdot \chi_1) \ell_R + \sqrt{\eta_L} \bar{t}^C_R (\gamma \cdot \chi_1) \ell_L\} \\ & + \Lambda_\nu \bar{b}^C_R (\gamma \cdot \chi_1) \nu_L + \text{H.c.},\end{aligned} \tag{14}$$

$$\begin{aligned}\mathcal{L} \supset\ & \bar{\Lambda}_\ell \{\epsilon_R \sqrt{\eta_R} \bar{b}_R (\gamma \cdot \chi_2) \ell_R + \sqrt{\eta_L} \bar{b}_L (\gamma \cdot \chi_2) \ell_L\} \\ & + \bar{\Lambda}_\nu \bar{t}_L (\gamma \cdot \chi_2) \nu_L + \text{H.c.},\end{aligned} \tag{15}$$

$$\mathcal{L} \supset \tilde{\Lambda}_\ell \{\sqrt{\eta_R} \bar{t}_R (\gamma \cdot \chi_5) \ell_R + \sqrt{\eta_L} \bar{t}_L (\gamma \cdot \chi_5) \ell_L\} + \text{H.c.}, \tag{16}$$

where we have suppressed the lepton generation index. We denote a generic charge $\pm n/3$ vLQ by χ_n. Here, η_L and $\eta_R = 1 - \eta_L$ are the charged lepton chirality fractions [89,97]. In Eq. (15), we have introduced a sign term $\epsilon_R = \pm 1$ to incorporate a possible relative sign between the left-handed and right-handed terms [see Eq. (7)]. We shall consider only real couplings in our analysis for simplicity.

As we did for the sLQs [89], here we identify some benchmark scenarios with the simplified models (see Table I). Each scenario corresponds to one of the realizable models described above [see Eqs. (1)–(13)]. Here, we have ignored any possible mixing among the vLQs. The BR for a

TABLE I. Summary of the nine benchmark scenarios considered. The branching ratio for a χ to decay to a top quark, β, is fixed for all models [Eqs. (1)–(13)], except for U_1 in the LCSS scenario ($\beta \leq 50\%$) and $V_2^{1/3}$ in the RLCSS/OS scenarios where $0 \leq \beta < 100\%$ (for $\beta = 100\%$, these two scenarios become the same as the RC scenario). The exceptional scenarios are marked by an asterisk. Here, λ is a generic free coupling parameter. For simplicity, we have chosen only this one coupling to control all of the nonzero new couplings in every benchmark. This essentially means also choosing β to be 50% in the exceptional scenarios.

		Simplified models [Eqs. (14)–(16)]			LQ models [Eqs. (1)–(13)]			
Benchmark scenario	Possible charge(s)	Type of LQ	Nonzero couplings equal to λ	Charged lepton chirality fraction	Type of LQ	Nonzero coupling equal to λ	Decay mode(s)	Branching ratios(s) $\{\beta, 1-\beta\}$
LC	1/3	χ_1	Λ_ℓ	$\eta_L = 1$	$\tilde{V}_2^{1/3}$	$\tilde{x}^{RL}_{2\,3j}$	$t\ell$	
	2/3	χ_2	$\bar{\Lambda}_\nu$	—	$(\tilde{V}_2^{-2/3})^\dagger$	$(\tilde{x}^{RL}_{2\,3j})^*$	$t\nu$	$\{100\%, 0\}$
	5/3	χ_5	$\tilde{\Lambda}_\ell$	$\eta_L = 1$	$U_3^{5/3}$	$\sqrt{2}x^{LL}_{3\,3j}$	$t\ell$	
LCSS*	2/3	χ_2	$\bar{\Lambda}_\ell = \bar{\Lambda}_\nu$	$\eta_L = 1$	U_1	$x^{LL}_{1\,3j}$	$\{t\nu, b\ell\}$	$\{50\%, 50\%\}$
LCOS			$\bar{\Lambda}_\ell = -\bar{\Lambda}_\nu$		$U_3^{2/3}$	$-x^{LL}_{3\,3j}$		
RC	1/3	χ_1	Λ_ℓ	$\eta_R = 1$	$V_2^{1/3}$	$x^{LR}_{2\,3j}$	$t\ell$	$\{100\%, 0\}$
	5/3	χ_5	$\tilde{\Lambda}_\ell$		$\tilde{U}_1$	$\tilde{x}^{RR}_{1\,3j}$		
RLCSS*	1/3	χ_1	$\Lambda_\ell = \Lambda_\nu$	$\eta_R = 1$	$V_2^{1/3}$	$x^{LR}_{2\,3j} = -x^{RL}_{2\,3j}$	$\{t\ell, b\nu\}$	$\{50\%, 50\%\}$
RLCOS*			$\Lambda_\ell = -\Lambda_\nu$		$V_2^{1/3}$	$x^{LR}_{2\,3j} = x^{RL}_{2\,3j}$		

χ to decay to a top quark, β, is fixed in all models [Eqs. (1)–(13)], except for two cases that we shall describe shortly. For simplicity, we choose only one free coupling λ parametrizing the nonzero new couplings in every benchmark scenario. (See the fourth and seventh columns of Table I. By doing this, we are essentially also choosing β to be 50% in the free β scenarios.)

(1) In the left coupling (LC) scenario, a χ can directly couple with left-handed leptons. We set λ equal to Λ_ℓ (for χ_1), $\tilde{\Lambda}_\ell$ (for χ_5), or $\bar{\Lambda}_\nu$ (for χ_2) and put all other couplings to zero. For χ_1 and χ_5 we set $\eta_L = 1$. Here, χ_1 represents a $\tilde{V}_2^{1/3}$ with $\Lambda_\ell = \tilde{x}^{RL}_{2\,3j}$, χ_5 represents a $U_3^{5/3}$ with $\tilde{\Lambda} = \sqrt{2}x^{LL}_{3\,3j}$, and χ_2 represents an anti-$\tilde{V}_2^{-2/3}$ with $\bar{\Lambda}_\nu = (\tilde{x}^{RL}_{2\,3j})^*$. In this scenario, a χ_1 or χ_5 decays to $t\ell$ pairs and a χ_2 decays to $t\nu$ pairs all of the time.

(2) If a χ_2 is of U_1 or $U_3^{2/3}$ type, it can also decay to a $b\ell$ pair. Hence, it is possible that a χ_2 couples with left-handed leptons but the BR for the decay $\chi_2 \to t\nu(\beta)$ is 50%. Such possibilities are captured in the left couplings with the same sign (LCSS) or the left couplings with opposite signs (LCOS) scenarios. The difference between these two comes from the different relative signs between the $\chi_2 b\ell$ and $\chi_2 t\nu$ couplings. In LCSS, the χ_2 behaves as a U_1 with $\bar{\Lambda}_\ell = \bar{\Lambda}_\nu = x^{LL}_{1\,3j}$, whereas in LCOS it behaves as a $U_3^{2/3}$ with $\bar{\Lambda}_\ell = -\bar{\Lambda}_\nu = -x^{LL}_{3\,3j}$. It is important to note that in the U_1 case, it is possible to have $\beta < 50\%$ if we consider a nonzero $x^{RR}_{1\,3j}$. This can be seen from Eq. (4). Unlike the sLQ case [89], the LCSS and LCOS scenarios for the vLQ yield the same single production cross section as there is no interference among the contributing diagrams.

(3) The right coupling (RC) scenario, where a LQ couples only to right-handed charged leptons, is exclusive to χ_1 and χ_5. Like the LC scenario, here we have $\beta = 100\%$. In this case a χ_1 behaves as a $V_2^{1/3}$ with $\Lambda_\ell = x^{LR}_{2\,3j}$ and a χ_5 behaves as a $\tilde{U}_1$ with $\tilde{\Lambda}_\ell = x^{RR}_{1\,3j}$.

(4) Unlike the sLQ ϕ_1 (see Ref. [89]), the χ_1 type vLQs (if it is $V_2^{1/3}$) can decay to both $t\ell$ and $b\nu$ pairs, provided Λ_ℓ and Λ_ν are both nonzero. We design two scenarios, namely, right (lepton) left (neutrino) couplings with the same sign (RLCSS) where $\chi_1 \equiv V_2^{1/3}$ with $\Lambda_\ell = \Lambda_\nu = x^{LR}_{2\,3j} = x^{RL}_{2\,3j}$, and right (lepton) left (neutrino) couplings with opposite signs (RLCOS) where $\chi_1 \equiv V_2^{1/3}$ with $\Lambda_\ell = -\Lambda_\nu = x^{LR}_{2\,3j} = x^{RL}_{2\,3j}$. In these two scenarios, β can be anything between 0 and 100% as both involve two independent couplings [$x^{LR}_{2\,3j}$ and $x^{RL}_{2\,3j}$; see Eq. (7)]. However, we consider only $\beta = 50\%$ for these benchmarks. We introduce these two benchmarks for completeness, though for our purpose these two are equivalent. As there is no interference contribution sensitive to this sign flip, all of the production processes would have the same cross sections in both scenarios.

Before we move on, we note that the kinetic terms for a vector leptoquark contains a free parameter, usually denoted as κ [94],

$$\mathcal{L} \supset -\frac{1}{2}\chi^\dagger_{\mu\nu}\chi^{\mu\nu} + M^2_\chi \chi^\dagger_\mu \chi^\mu - ig_s \kappa \chi^\dagger_\mu T^a \chi_\nu G^{a\mu\nu}, \quad (17)$$

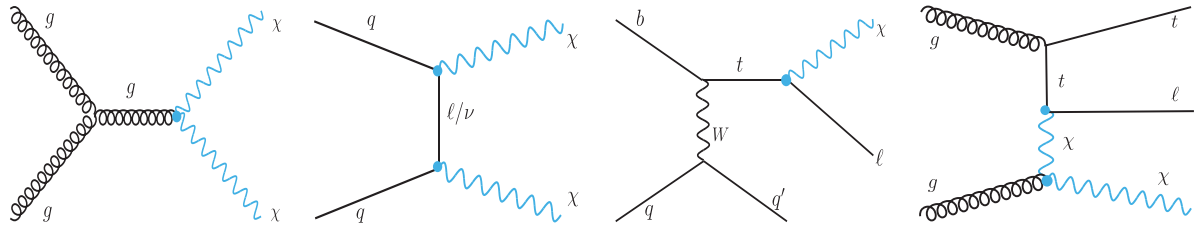

FIG. 1. Representative Feynman diagrams for the LQ production at the LHC. Panels (a) and (b) show pair production processes and panels (c) and (d) show single production processes.

where $\chi_{\mu\nu}$ stands for the field-strength tensor of χ. This parameter κ can change pairs and (interestingly) some single production cross sections through the modification of the $\chi\chi g$ vertex.[2] We take two benchmark cases with $\kappa = 0$ and $\kappa = 1$ in our analysis.

III. LHC PHENOMENOLOGY AND SEARCH STRATEGY

We keep our computational setup the same as before [89]. We use FeynRules [99] to create the UFO [100] model files for the Lagrangians in Eqs. (14)–(16). Both the signal and background events are generated in MADGRAPH5 [101] at the leading order (LO). We include higher-order corrections to the background processes with QCD K factors wherever available. For VLQs, higher-order K factors for signal processes are not yet known. We use NNPDF2.3LO [102] parton distribution functions with default dynamical renormalization and factorization scales to generate events in MADGRAPH5, and then pass them through PYTHIA6 [103] for showering and hadronization. Detector effects are simulated using DELPHES3 [104] with the default CMS card. Fat jets are reconstructed from DELPHES tower objects using the Cambridge-Achen [105] clustering algorithm (with $R = 1.5$) in FASTJET [106]. We reconstruct hadronic tops from fat jets with HEPTOPTAGGER [107] with default parameters except for the top-mass window which we relax a little to 80 GeV from the default 50 GeV to keep more signal events.

A. Production at the LHC

The vLQs would be produced resonantly at the LHC through the pair and single production channels. The dominant pair production diagrams are free of the new couplings and depend only on the universal strong coupling (there are diagrams with t-channel lepton exchange that involve new couplings [see Fig. 1(b)], but their contribution to the total pair production cross section is small [97]); hence, the process is mostly model independent up to a choice of κ. The pair production would lead to the following final states:

$$pp \to \left\{ \begin{array}{l} \chi_1\chi_1 \to (t\ell)(t\ell)/(t\ell)(b\nu)/(b\nu)(b\nu) \\ \chi_2\chi_2 \to (t\nu)(t\nu)/(t\nu)(b\ell)/(b\ell)(b\ell) \\ \chi_5\chi_5 \to (t\ell)(t\ell) \end{array} \right\}. \tag{18}$$

Here, as we did for the sLQs [89], we ignore those channels with no top quark and consider only symmetric channels, i.e., both of the vLQs decay to the same final state. Constraining ourselves to such channels will restrict the possible SM backgrounds and make our signal easier to detect. It is generally believed that the symmetric modes have good discovery prospects [108].[3] With these considerations, we are now left with only the $(t\ell)(t\ell)$ (for χ_1 or χ_5) and $(t\nu)(t\nu)$ (for χ_2) channels.

With similar consideration for the single production processes, where a LQ is produced in association with a lepton and either a jet or a top quark, the possible final states are given as

$$pp \to \left\{ \begin{array}{l} \chi_1 t\ell \to (t\ell)t\ell \\ \chi_1 \ell j \to (t\ell)\ell j \end{array} \right\}, \tag{19}$$

$$pp \to \left\{ \begin{array}{l} \chi_2 t\nu \to (t\nu)t\nu \\ \chi_2 \nu j \to (t\nu)\nu j \end{array} \right\}, \tag{20}$$

$$pp \to \left\{ \begin{array}{l} \chi_5 t\ell \to (t\ell)t\ell \\ \chi_5 \ell j \to (t\ell)\ell j \end{array} \right\}. \tag{21}$$

In Fig. 1 we show some representative Feynman diagrams of the pair and single productions of vLQs.

In Fig. 2 we show the parton-level cross sections of different production processes of χ_1 [Figs. 2(a)–2(b)], χ_2 [Figs. 2(c)–2(d)], and χ_5 [Figs. 2(e)–2(f)] as functions of their masses. The single production cross sections scale as λ^2. Here they are computed for different benchmark

[2]Similar modifications are also possible for other gauge bosons [92,93]. However, we ignore direct electroweak $\chi - V$ couplings in our analysis.

[3]The asymmetric modes (where the two LQs decay differently) have not been used for LQ searches so far. For some LQ models, asymmetric channels could provide a better reach than symmetric channels and, therefore, require a separate dedicated analysis [109].

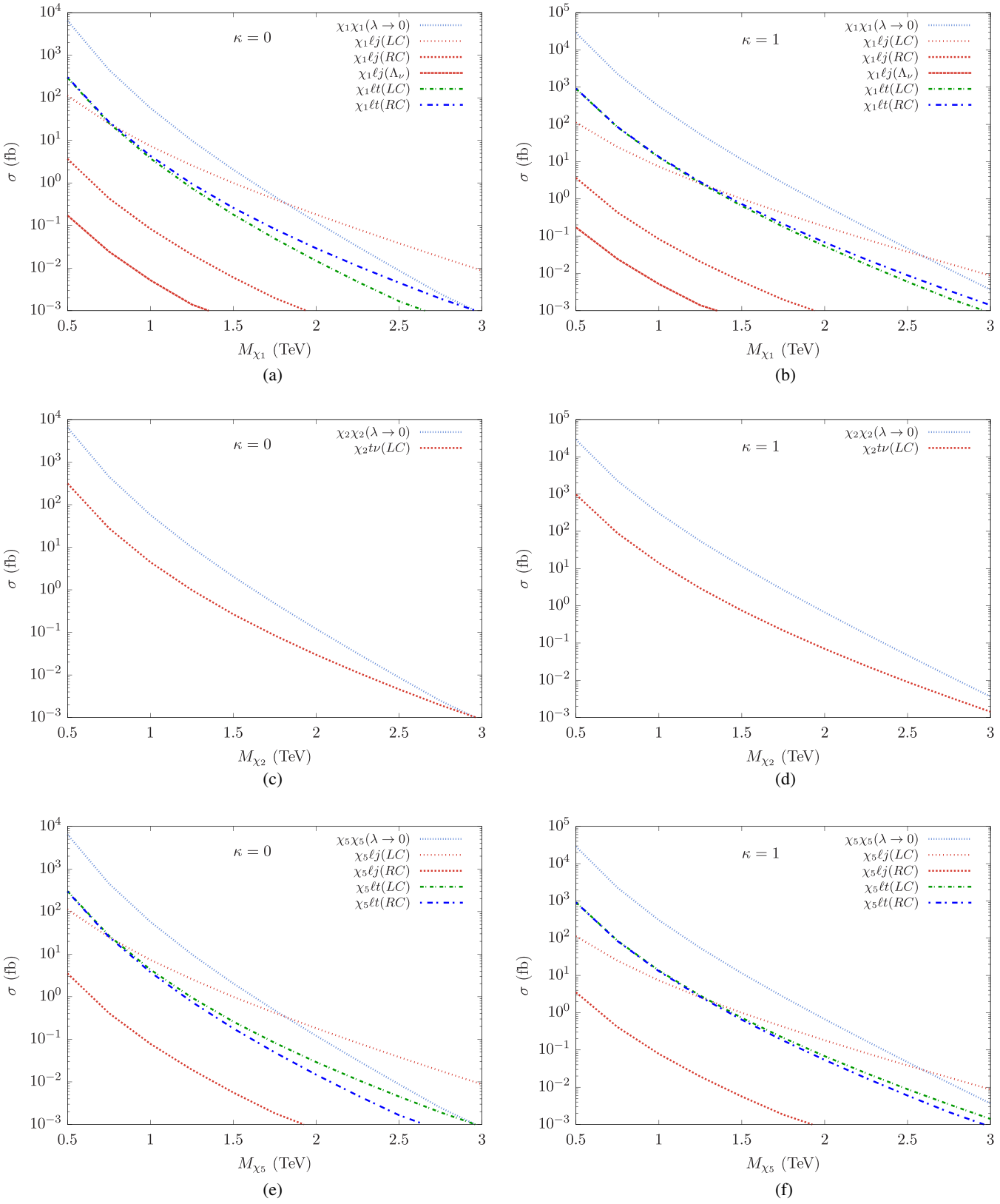

FIG. 2. The parton-level cross sections of different production channels of χ_1 [(a) and (b)], χ_2 [(c) and (d)], and χ_5 [(e) and (f)] at the 14 TeV LHC as functions of M_{χ_n}. The single production cross sections are computed for a benchmark coupling $\lambda = 1$ (see Table I). Here, ℓ stands for either an electron or a muon and the j in the single production processes includes all of the light jets as well as b jets. Their cross sections are generated with a cut on the transverse momentum of the jet, $p_T^j > 20$ GeV.

scenarios with a reference value $\lambda = 1$. We see that in the LC scenario with $\kappa = 0$, the single production cross section $\sigma(pp \to \chi_1 \ell j)$ overtakes the pair production cross section at about 1.8 TeV, while $\sigma(pp \to \chi_1 t\ell)$ always remains smaller. For $\kappa = 1$, the pair production cross section increases, moving the crossover point with $\sigma(pp \to \chi_1 \ell j)$ to about 2.6 TeV. Interestingly, we find that $\sigma(pp \to \chi_1 t\ell)$ depends on the choice of κ despite being a single production process as it contains the κ-dependent $\chi_1\chi_1 g$ vertex. In the RC scenario, $\sigma(pp \to \chi_1 \ell j)$ is reduced by almost 2 orders of magnitude compared to that in the LC scenario. This happens because in the RC scenario, a χ_1 couples to a right-handed top that comes from another left-handed top generated in the charged-current interaction through a chirality flip. If the Λ_ν coupling alone is turned on, the cross section for the $pp \to \chi_1 \ell j$ process is negligible [see Figs. 2(a)–2(b)]. (Note, however, that a nonzero Λ_ν can still affect the BRs. For example, we can consider RLCSS and RLCOS scenarios where the BRs for the $\chi_1 \to t\ell$ and $\chi_1 \to b\nu$ modes are 50% each.) Now, because of the small contribution from the Λ_ν-dependent diagrams and the fact that there is no interference in both the RLCSS and RLCOS scenarios, the $pp \to \chi_1 \ell j$ process would have the same cross section as in the RC scenario. For χ_2, pair production $pp \to \chi_2\chi_2$ always dominates over single production $pp \to \chi_2 t\nu$ up to a mass of 3 TeV with $\lambda = 1$ coupling for both $\kappa = 0$ and $\kappa = 1$. In this case, we obtain a tt plus large $\not{E}_T$ signature, which was analyzed in Ref. [90]. The χ_5 vLQ is similar to the χ_1 and yields similar signatures at the colliders.

The distinctive feature of our signal is the presence of boosted top quarks and high-p_T charged leptons. In symmetric modes, we have at least one top quark in the final state for single production while the pair production gives rise to two top quarks. In both cases, we have two high-p_{T} charged leptons. Therefore, as already indicated in the Introduction, we combine events from both pair and single productions by demanding at least one top jet (a hadronically decaying top quark forming a fat jet) and exactly two high-p_{T} same-flavor-opposite-sign (SFOS) leptons in the final state to enhance the signal sensitivity. Note that the same final state can arise from both pair and single production processes. For example, the $t\ell t\ell$ state can come from both $pp \to \chi_{1,5}\chi_{1,5}$ and $pp \to \chi_{1,5} t\ell$ processes (see Fig. 1). This can lead to double counting the contribution of some diagrams while generating signal events. One can avoid this by ensuring that both χ and $\chi^\dagger$ are not on-shell simultaneously in any single production event [97].

B. Backgrounds and selection

Since the topology of the vLQ signal is identical to that of the sLQ signal [i.e., at least one (hadronic) top fat jet and exactly two high-p_{T} SFOS leptons], our background analysis essentially remains the same as before [89]. Therefore, we refer the reader to the earlier paper for a detailed discussion on the possible SM background processes; here, we present the gist of our discussions found there. The dominant SM background processes for our desired signal can arise from processes with two leptons and significant cross sections at the LHC. The top-like fat jet can appear from either an actual top quark decaying hadronically or a bunch of QCD/non-QCD jets mimicking its signature. We find that $pp \to Z + \text{jets}$ and $pp \to tt + \text{jets}$ processes contribute significantly to the background. The single top, diboson, and ttV ($V = W, Z$) production processes are subdominant. There are SM processes with large cross sections, e.g., $pp \to W + \text{jets} \to \ell\nu + \text{jets}$ that can in principle act as backgrounds because of a jet mimicking a lepton. However, we found that these processes actually contribute negligibly, thanks to a very small misidentification efficiency.

TABLE II. Total cross sections without any cut for SM background processes considered in our analysis. The higher-order QCD cross sections are taken from the literature and are shown in the last column. We use these cross sections to compute the K factors, which multiply the LO cross sections to include higher-order effects.

Background processes		σ (pb)	QCD Order
$V + \text{jets}$ [110,111]	$Z + \text{jets}$	6.33×10^4	NNLO
	$W + \text{jets}$	1.95×10^5	NLO
$VV + \text{jets}$ [112]	$WW + \text{jets}$	124.31	NLO
	$WZ + \text{jets}$	51.82	NLO
	$ZZ + \text{jets}$	17.72	NLO
Single t [113]	tW	83.1	$\mathrm{N^2LO}$
	tb	248.0	$\mathrm{N^2LO}$
	tj	12.35	$\mathrm{N^2LO}$
tt [114]	$tt + \text{jets}$	988.57	$\mathrm{N^3LO}$
ttV [115]	ttZ	1.045	NLO + NNLL
	ttW	0.653	NLO + NNLL

In Table II we list the relevant SM processes and their higher-order cross sections. We consider these backgrounds after adjusting with appropriate K factors to include higher-order effects. Although the bare cross sections (i.e., without any cut) of some background processes are seemingly huge, we control them by applying strong selection cuts. These cuts are designed in such a way that they would drastically reduce the background without harming the signal much since our signal possesses specific kinematic features that are very different from the backgrounds. However, some backgrounds are so big at the beginning (e.g., $Z + \text{jets}$) that in order to save computation time and have better statistics, we apply the following strong cuts at the generation level:

(1) $p_{\mathrm{T}}(\ell_1) > 250$ GeV.

(2) Invariant mass $M(\ell_1, \ell_2) > 115$ GeV (Z-mass veto).

Here ℓ_i denotes the ith p_{T}-ordered lepton (e/μ). After generating events with the above generation-level cuts, we

apply the following final selection criteria sequentially on the signal and background events at the analysis level:

(1) $\mathcal{C}_1$:
   (a) Minimum one top jet (obtained from HEPTOPTAGGER) with $p_T(t_h) > 135$ GeV.
   (b) Exactly two SFOS leptons with $p_T(\ell_1) > 400$ GeV and $p_T(\ell_2) > 200$ GeV and pseudorapidity $|\eta(\ell)| < 2.5$. For e, we consider the barrel–end cap cut on η between 1.37 and 1.52.
   (c) Invariant mass of the lepton pair $M(\ell_1, \ell_2) > 120$ GeV (Z veto).
   (d) The missing energy $\not{E}_T < 200$ GeV.

(2) $\mathcal{C}_2$: The scalar sum of the transverse p_T of all visible objects, $S_T > 1.2 \times \text{Min}(M_\chi, 1750)$ GeV.

(3) $\mathcal{C}_3$: $\text{Max}(M(\ell_1, t)$ OR $M(\ell_2, t)) > 0.8 \times \text{Min}(M_\chi, 1750)$ GeV.

IV. DISCOVERY POTENTIAL

We use the following formula to estimate the signal significance $\mathcal{Z}$:

$$\mathcal{Z} = \sqrt{2(N_S + N_B)\ln\left(\frac{N_S + N_B}{N_B}\right) - 2N_S}, \quad (22)$$

where the number of signal and background events surviving the final selection cuts (as listed in the previous section) are denoted by N_S and N_B, respectively. In Fig. 3

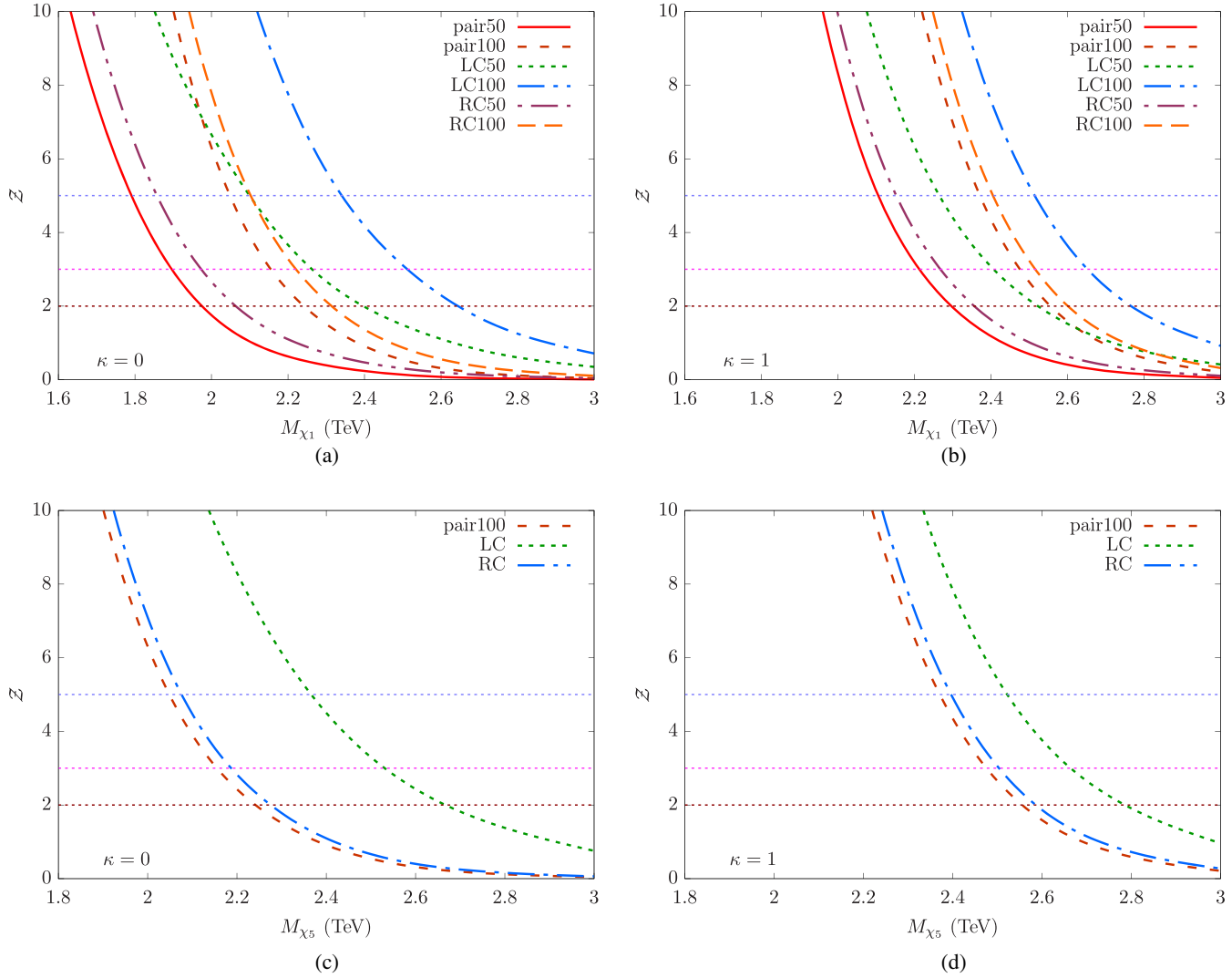

FIG. 3. Expected significance $\mathcal{Z}$ in units of standard deviation σ for observing the χ_1 (a) [$\kappa = 0$], (b) [$\kappa = 1$] and χ_5 (c) [$\kappa = 0$], (d) [$\kappa = 1$] signals over the SM backgrounds. They are plotted as functions of their masses for 3 ab^{-1} of integrated luminosity at the 14 TeV HL-LHC for different coupling scenarios in the electron mode. We use the combined pair and single productions for the signals in the LC and RC scenarios. We also show the pair production significance for 50% and 100% BRs in the $\chi \to t\ell$ decay mode. We have considered $\lambda = 1$ when computing the signals.

TABLE III. The mass limits corresponding to 5σ (discovery), 3σ, and 2σ (exclusion) significances ($\mathcal{Z}$) for observing the (a) χ_1 and (b) χ_5 signals over the SM backgrounds for 3 ab^{-1} integrated luminosity at the 14 TeV LHC with combined and pair-production-only signals. Here, LC (RS) stands for LC100 (RC100).

	Limit on M_χ (TeV)																	
	$\kappa=0$									$\kappa=1$								
	χ_1						χ_5			χ_1						χ_5		
	Combined				Pair		Combined		Pair	Combined				Pair		Combined		Pair
Significance $\mathcal{Z}$	LC50	LC	RC50	RC	BR = 0.5	BR = 1	LC	RC	BR = 1	LC50	LC	RC50	RC	BR = 0.5	BR = 1	LC	RC	BR = 1
5	2.10	2.34	1.85	2.10	1.79	2.05	2.36	2.07	2.04	2.26	2.51	2.14	2.40	2.10	2.36	2.52	2.39	2.36
3	2.25	2.51	1.97	2.22	1.89	2.15	2.52	2.18	2.15	2.40	2.65	2.26	2.51	2.21	2.47	2.66	2.50	2.47
2	2.39	2.64	2.06	2.31	1.97	2.23	2.66	2.27	2.23	2.52	2.76	2.35	2.59	2.29	2.55	2.78	2.58	2.55

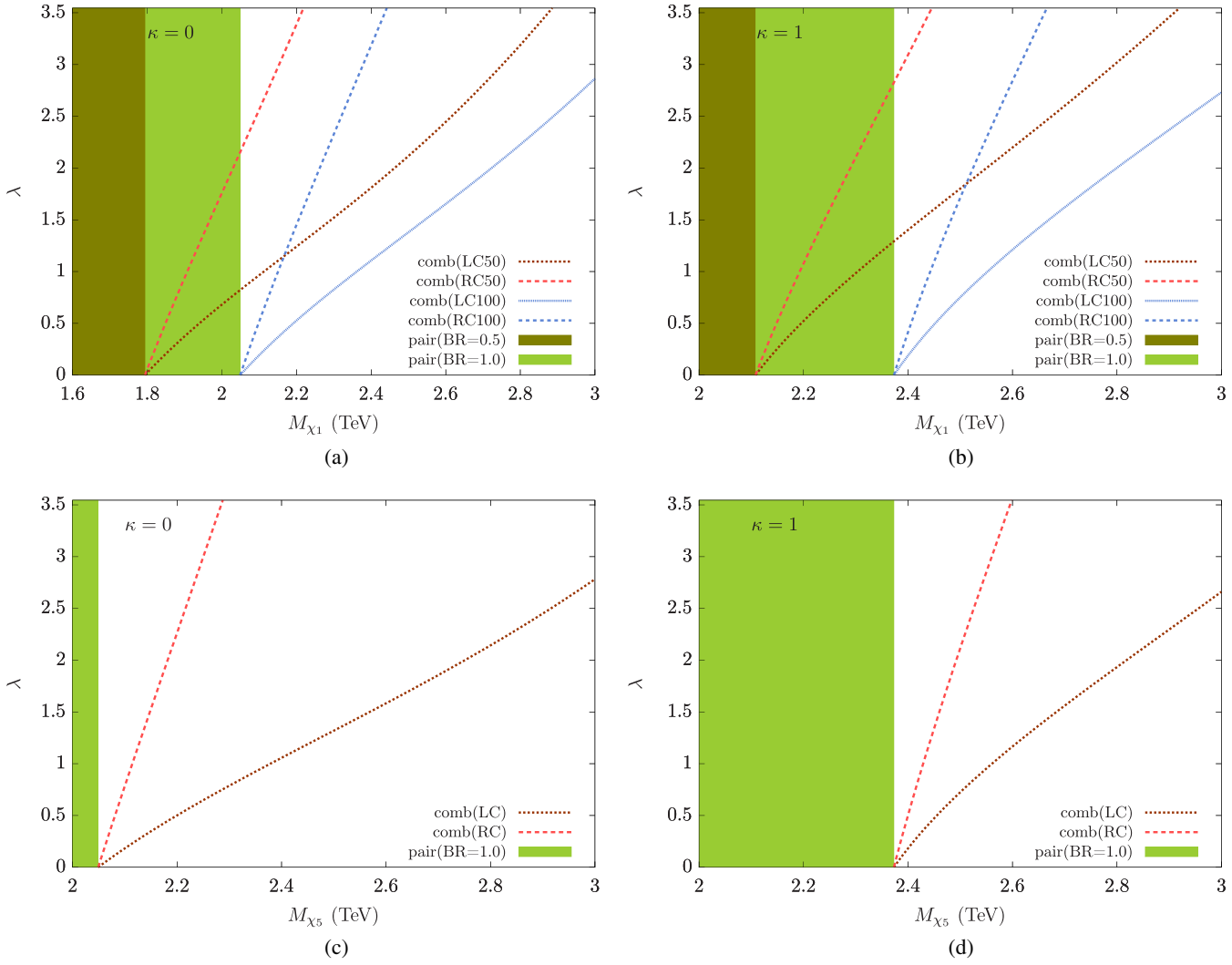

FIG. 4. The 5σ discovery reaches in the $\lambda - M_\chi$ planes for χ_1 with (a) $\kappa = 0$ and (b) $\kappa = 1$ and for χ_5 with (c) $\kappa = 0$ and (d) $\kappa = 1$. These plots show the smallest λ needed to observe χ_1 and χ_5 signals with 5σ significance for a range of M_χ with 3 ab^{-1} of integrated luminosity. The pair-production-only regions for 50% and 100% BRs in the $\chi \to t\ell$ decay mode are shown with shades of green. Since the pair production is insensitive to λ, a small coupling is sufficient to attain 5σ significance within the green regions.

we show the expected significance as a function of vLQ masses. As discussed earlier, the choice of κ affects the pair and some single productions. In Figs. 3(a) and 3(b) we present $\mathcal{Z}$ for χ_1 with $\kappa = 0$ and $\kappa = 1$, respectively. Similarly, Figs. 3(c) and 3(d) are for χ_5. These curves are obtained for the 14 TeV LHC with 3 ab^{-1} of integrated luminosity. We have used $\lambda = 1$ to estimate the significance for the combined signal (i.e., the pair and single production events together). We note the following points:

(i) The LC100 (RC100) curves for χ_1 and the LC (RC) curves for χ_5 represent the significances in the LC (RC) scenario where the BR of the $\chi_1 \to t\ell$ decay is 100%.

(ii) For χ_1, the LC50 and RC50 curves represent the cases where the BR of $\chi_1 \to t\ell$ decay mode is 50%. Although they are not realized in the LC and RC scenarios, such a situation is possible if there are other decay modes of χ_1 (which play no role in our analysis beyond modifying the BR). Hence, we show these plots to give some estimates of how the significance would vary with the BR.

(iii) For comparison, we also show the expected significance obtained with only the pair production events for the 50% and 100% BR cases. For instance, for 100% BR in the $\chi_1 \to t\ell$ mode, the HL-LHC (3 ab^{-1}) discovery mass reach (i.e., $\mathcal{Z} = 5\sigma$) with only pair production is about 2.05 (2.35) TeV for $\kappa = 0$ ($\kappa = 1$).

(iv) When the LC coupling is unity, the discovery reach goes up to 2.35(2.50) TeV once the single production processes are included. However, in the RC scenario the improvement is minor. This happens because $\sigma(pp \to \chi_1 \ell j)$ is larger in the LC scenario than that in the RC scenario.

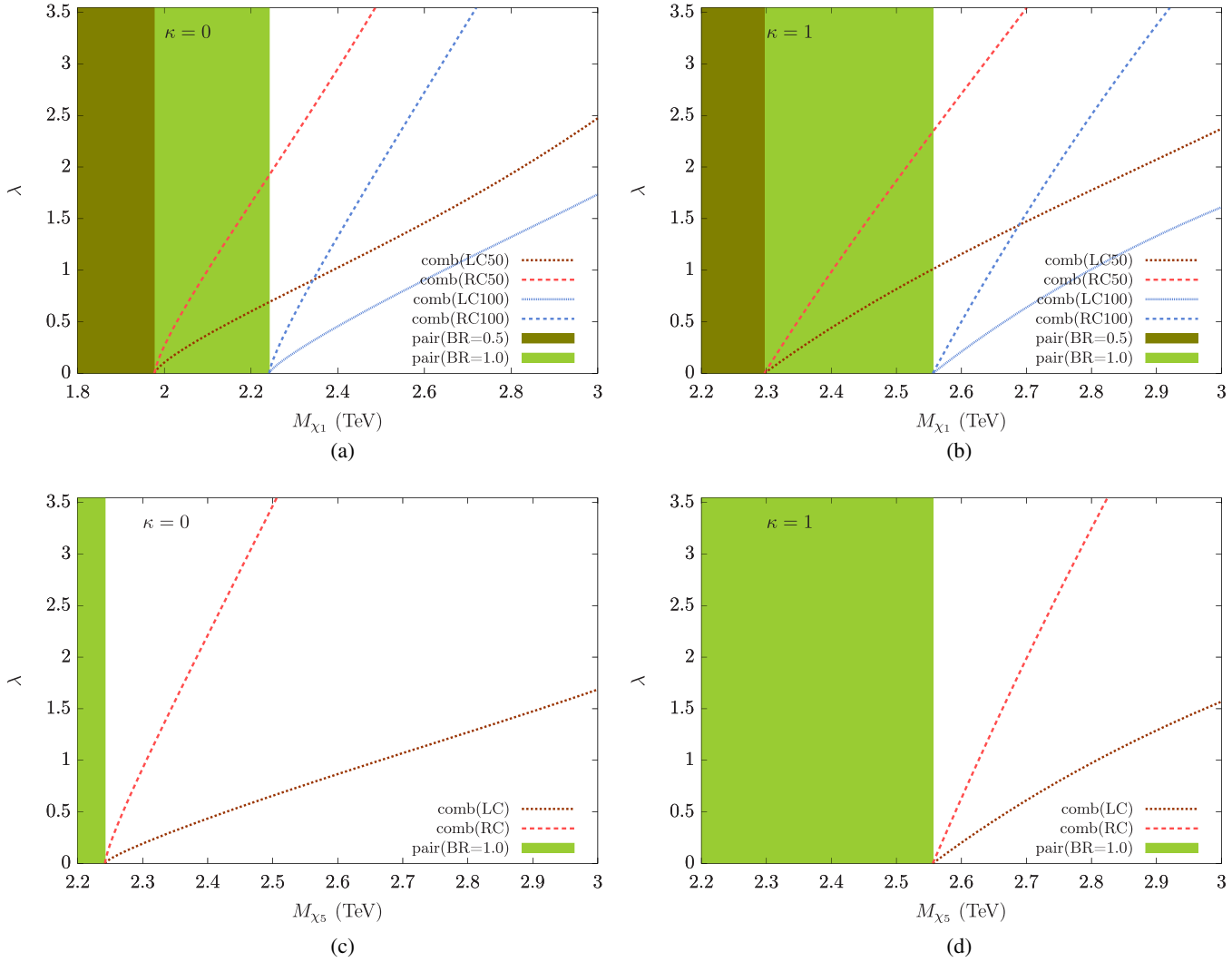

FIG. 5. The 2σ exclusion limits in the $\lambda - M_\chi$ planes for χ_1 with (a) $\kappa = 0$ and (b) $\kappa = 1$ and for χ_5 with (c) $\kappa = 0$ and (d) $\kappa = 1$. These plots show the smallest λ that can be excluded by the HL-LHC with 3 ab^{-1} of integrated luminosity. The pair-production-only regions for 50% and 100% BRs in the $\chi \to t\ell$ decay mode are shown with green shades.

(v) Unlike the scalar case, there is no interference among the different signal diagrams, and hence the signal significances in the RLCSS or RLCOS benchmarks are the same as that in the RC scenario.

(vi) In Figs. 3(c) and 3(d) we observe that the maximum reach for χ_5 comes from the combined LC scenario. The values are 2.35 and 2.50 TeV for $\kappa = 0$ and $\kappa = 1$, respectively. There is a suppression in the RC channel for a similar reason as for χ_1, a χ_5 LQ also couples to a right chiral top.

In Table III we collect all of the numbers for $\mathcal{Z} = 2\sigma$, 3σ, and 5σ.

Since we can parametrize the combined signal cross section for any M_χ as

$$\sigma_{\text{signal}} \approx \sigma_{\text{pair}}(M_\chi) + \lambda^2 \sigma_{\text{single}}(\lambda = 1, M_\chi), \qquad (23)$$

the combined signal cross section increases with λ for any fixed M_χ. By recasting the figures shown in Fig. 3, which are for $\lambda = 1$, we can obtain the reach in the $\lambda - M_\chi$ plane, as we show in Figs. 4 and 5. We show the 5σ discovery curves in Fig. 4, while the 2σ exclusion curves are displayed in Fig. 5. These plots show the lowest value of λ required to observe the vLQ signal for a varying M_χ with 5σ confidence level for discovery. For the exclusion plots, all points above the curves can be excluded at the 95% confidence level at the HL-LHC.

V. SUMMARY AND CONCLUSIONS

Usually, in the direct LQ searches, it is assumed that LQs only couple to quarks and leptons of the same generation. Collider signatures of TeV-scale LQs with large cross-generational couplings, motivated by the persistent flavor anomalies, are completely different than what is considered in the usual LQ searches at the LHC. It is then important to explore these possibilities in detail. In a previous paper [89], we investigated the HL-LHC prospects of all scalar LQ models within the Buchmüller-Rückl-Wyler classifications [91] that would produce *boosted-t+ high-*$p_{\text{T}} - \ell$ signatures at the LHC. In this follow-up paper, we investigated the case for the vector LQs with the same signature. The vLQs that decay to a top quark can have three possible electric charges: $\pm 1/3$, $\pm 2/3$, and $\pm 5/3$. Among these, our primary focus was on the charge $\pm 1/3$, $\pm 5/3$ vLQs that can decay to a top quark and an electron or a muon, as a unique top-lepton resonance system would appear from the decays of these LQs.

In this paper, we introduced some simple phenomenological Lagrangians. These simple models can cover the relevant parameter spaces of the full models described in Refs. [91,94]. In this simplified framework, we studied the pair and single production channels of vector LQs at the LHC. Pair production of the vLQs produces final states with two boosted top quarks and two high-p_T leptons and determines the LHC discovery reach in the low-mass region. On the other hand, the single production processes produce final states with at least one boosted top quark and two high-p_T leptons. We observed two interesting points about single production. 1) Despite considering vLQ couplings with only third-generation quarks, we saw that the single production cross sections are not necessarily very small, provided, of course, the new couplings controlling them are not negligible. 2) Like the pair production, some single production processes can also depend on the parameter κ that appears in the gluon-vector LQ coupling. In some scenarios, for order-one new coupling(s), the single production would control the LHC reach in the high-mass region.

We adopted a search strategy of selecting events with at least one boosted hadronic top quark and exactly two high-p_{T} leptons of the same flavor and opposite sign. This combines events from the pair and single productions and, therefore, enhances the discovery reach by about 300 GeV from the usual pair production searches at the LHC. Our results show that charge $1/3$ and $5/3$ vector LQs can be probed up to 2.35 (2.50) TeV for 100% branching ratio in the $t\ell$ decay mode for $\kappa = 0$ ($\kappa = 1$) and order-one new couplings at the 14 TeV LHC with 3 ab^{-1} of integrated luminosity with 5σ significance. Alternately, in the absence of their discoveries, they can be excluded up to 2.65 (2.75) TeV at the 95% confidence limit. Since the single production cross sections scale as λ^2, we also showed how the discovery/exclusion reach would vary with λ within its perturbative domain.

Comparing with the results in Ref. [89], we saw that in general it may be possible for the LHC to discover/exclude heavier vLQs than sLQs for comparable parameters. For example, for $\lambda = 1$ the 5σ discovery reach for χ_5 goes up to 2.35 TeV ($\kappa = 0$) in the LC scenario. This is higher than the 1.75 TeV reach in the LC scenario for ϕ_5 (or even 1.95 TeV in the RC scenario). Similar observations can be made for other LQs/scenarios too. Of course, in the case of vLQs, the additional parameter κ can enhance the reaches even more; for χ_5 in the LC scenario, it increases to 2.5 TeV. There is no such parameter in the case of sLQs; in this regard, the sLQ pair production process is more model independent (i.e., QCD driven) than that for vLQs. Also, for some sLQs the relative signs between new physics couplings are important as they affect the single production cross sections through interference among different signal diagrams. This happens for ϕ_1 whose single production cross sections in the LCSS and LCOS scenarios differ significantly. However, there is no such interference for vLQs; for example, the χ_1 single production cross section is the same in the RLCSS and RLCOS scenarios. Of course, for both sLQs as well as vLQs, single production processes do play an important role in determining the LHC discovery/exclusion reaches even though we considered only third-generation quarks coupling with the LQs. It would be interesting to investigate ways to distinguish sLQs and vLQs with such similar signatures at the LHC. Finally, we

point out that in these two papers we have presented simplified models for all possible LQs that couple with the top quark and leptons. These simplified modes are suitable for bottom-up/experimental studies and can be easily mapped to the full models.

ACKNOWLEDGMENTS

A. B. and S. M. acknowledge financial support from the Science and Engineering Research Board (SERB), DST, India under Grant No. ECR/2017/000517.

[1] J. P. Lees *et al.* (*BABAR* Collaboration), Evidence for an Excess of $\bar{B} \to D^{(*)}\tau^-\bar{\nu}_\tau$ Decays, Phys. Rev. Lett. **109**, 101802 (2012).

[2] J. P. Lees *et al.* (*BABAR* Collaboration), Measurement of an excess of $\bar{B} \to D^{(*)}\tau^-\bar{\nu}_\tau$ decays and implications for charged Higgs Bosons, Phys. Rev. D **88**, 072012 (2013).

[3] R. Aaij *et al.* (LHCb Collaboration), Measurement of the Ratio of Branching Fractions $\mathcal{B}(\bar{B}^0 \to D^{*+}\tau^-\bar{\nu}_\tau)/\mathcal{B}(\bar{B}^0 \to D^{*+}\mu^-\bar{\nu}_\mu)$, Phys. Rev. Lett. **115**, 111803 (2015); Phys. Rev. Lett. **115**, 159901(E) (2015).

[4] R. Aaij *et al.* (LHCb Collaboration), Measurement of the Ratio of the $B^0 \to D^{*-}\tau^+\nu_\tau$ and $B^0 \to D^{*-}\mu^+\nu_\mu$ Branching Fractions Using Three-Prong τ-Lepton Decays, Phys. Rev. Lett. **120**, 171802 (2018).

[5] R. Aaij *et al.* (LHCb Collaboration), Test of lepton flavor universality by the measurement of the $B^0 \to D^{*-}\tau^+\nu_\tau$ branching fraction using three-prong τ decays, Phys. Rev. D **97**, 072013 (2018).

[6] M. Huschle *et al.* (Belle Collaboration), Measurement of the branching ratio of $\bar{B} \to D^{(*)}\tau^-\bar{\nu}_\tau$ relative to $\bar{B} \to D^{(*)}\ell^-\bar{\nu}_\ell$ decays with hadronic tagging at Belle, Phys. Rev. D **92**, 072014 (2015).

[7] S. Hirose *et al.* (Belle Collaboration), Measurement of the τ Lepton Polarization and $R(D^*)$ in the Decay $\bar{B} \to D^*\tau^-\bar{\nu}_\tau$, Phys. Rev. Lett. **118**, 211801 (2017).

[8] S. Hirose *et al.* (Belle Collaboration), Measurement of the τ lepton polarization and $R(D^*)$ in the decay $\bar{B} \to D^*\tau^-\bar{\nu}_\tau$ with one-prong hadronic τ decays at Belle, Phys. Rev. D **97**, 012004 (2018).

[9] A. Abdesselam *et al.* (Belle Collaboration), Measurement of $\mathcal{R}(D)$ and $\mathcal{R}(D^*)$ with a semileptonic tagging method, arXiv:1904.08794.

[10] D. Bigi and P. Gambino, Revisiting $B \to D\ell\nu$, Phys. Rev. D **94**, 094008 (2016).

[11] F. U. Bernlochner, Z. Ligeti, M. Papucci, and D. J. Robinson, Combined analysis of semileptonic B decays to D and D^*: $R(D^{(*)})$, $|V_{cb}|$, and new physics, Phys. Rev. D **95**, 115008 (2017); Phys. Rev. D **97**, 059902 (2018).

[12] D. Bigi, P. Gambino, and S. Schacht, $R(D^*)$, $|V_{cb}|$, and the Heavy Quark Symmetry relations between form factors, J. High Energy Phys. 11 (2017) 061.

[13] S. Jaiswal, S. Nandi, and S. K. Patra, Extraction of $|V_{cb}|$ from $B \to D^{(*)}\ell\nu_\ell$ and the Standard Model predictions of $R(D^{(*)})$, J. High Energy Phys. 12 (2017) 060.

[14] R. Aaij *et al.* (LHCb Collaboration), Differential branching fractions and isospin asymmetries of $B \to K^{(*)}\mu^+\mu^-$ decays, J. High Energy Phys. 06 (2014) 133.

[15] R. Aaij *et al.* (LHCb Collaboration), Test of Lepton Universality Using $B^+ \to K^+\ell^+\ell^-$ Decays, Phys. Rev. Lett. **113**, 151601 (2014).

[16] R. Aaij *et al.* (LHCb Collaboration), Angular analysis of the $B^0 \to K^{*0}\mu^+\mu^-$ decay using 3 fb^{-1} of integrated luminosity, J. High Energy Phys. 02 (2016) 104.

[17] R. Aaij *et al.* (LHCb Collaboration), Test of lepton universality with $B^0 \to K^{*0}\ell^+\ell^-$ decays, J. High Energy Phys. 08 (2017) 055.

[18] R. Aaij *et al.* (LHCb Collaboration), Search for Lepton-Universality Violation in $B^+ \to K^+\ell^+\ell^-$ Decays, Phys. Rev. Lett. **122**, 191801 (2019).

[19] G. Hiller and F. Kruger, More model-independent analysis of $b \to s$ processes, Phys. Rev. D **69**, 074020 (2004).

[20] M. Bordone, G. Isidori, and A. Pattori, On the Standard Model predictions for R_K and R_{K^*}, Eur. Phys. J. C **76**, 440 (2016).

[21] R. Aaij *et al.* (LHCb Collaboration), Measurement of the Ratio of Branching Fractions $\mathcal{B}(B_c^+ \to J/\psi\tau^+\nu_\tau)/\mathcal{B}(B_c^+ \to J/\psi\mu^+\nu_\mu)$, Phys. Rev. Lett. **120**, 121801 (2018).

[22] G. W. Bennett *et al.* (Muon g-2 Collaboration), Final report of the Muon E821 anomalous magnetic moment measurement at BNL, Phys. Rev. D **73**, 072003 (2006).

[23] Y. Sakaki, M. Tanaka, A. Tayduganov, and R. Watanabe, Testing leptoquark models in $\bar{B} \to D^{(*)}\tau\bar{\nu}$, Phys. Rev. D **88**, 094012 (2013).

[24] R. Mohanta, Effect of scalar leptoquarks on the rare decays of B_s meson, Phys. Rev. D **89**, 014020 (2014).

[25] S. Sahoo and R. Mohanta, Scalar leptoquarks and the rare B meson decays, Phys. Rev. D **91**, 094019 (2015).

[26] U. K. Dey and S. Mohanty, Constraints on Leptoquark models from IceCube data, J. High Energy Phys. 04 (2016) 187.

[27] T. Mandal, S. Mitra, and S. Seth, Pair production of scalar Leptoquarks at the LHC to NLO parton shower accuracy, Phys. Rev. D **93**, 035018 (2016).

[28] M. Freytsis, Z. Ligeti, and J. T. Ruderman, Flavor models for $\bar{B} \to D^{(*)}\tau\bar{\nu}$, Phys. Rev. D **92**, 054018 (2015).

[29] S. Sahoo and R. Mohanta, Study of the rare semileptonic decays $B_d^0 \to K^* l^+ l^-$ in scalar leptoquark model, Phys. Rev. D **93**, 034018 (2016).

[30] S. Sahoo and R. Mohanta, Leptoquark effects on $b \to s\nu\bar{\nu}$ and $B \to Kl^+l^-$ decay processes, New J. Phys. **18**, 013032 (2016).

[31] U. Aydemir, SO(10) grand unification in light of recent LHC searches and colored scalars at the TeV-scale, Int. J. Mod. Phys. A **31**, 1650034 (2016).

[32] S. Sahoo and R. Mohanta, Lepton flavor violating B meson decays via a scalar leptoquark, Phys. Rev. D **93**, 114001 (2016).

[33] U. Aydemir and T. Mandal, LHC probes of TeV-scale scalars in SO(10) grand unification, Adv. High Energy Phys. **2017**, 7498795 (2017).

[34] D. Das, C. Hati, G. Kumar, and N. Mahajan, Towards a unified explanation of $R_{D^{(*)}}$, R_K and $(g-2)_\mu$ anomalies in a left-right model with leptoquarks, Phys. Rev. D **94**, 055034 (2016).

[35] S. Sahoo and R. Mohanta, Effects of scalar leptoquark on semileptonic Λ_b decays, New J. Phys. **18**, 093051 (2016).

[36] D. Bečirević, N. Košnik, O. Sumensari, and R. Z. Funchal, Palatable leptoquark scenarios for lepton flavor violation in exclusive $b \to s\ell_1\ell_2$ modes, J. High Energy Phys. 11 (2016) 035.

[37] P. Bandyopadhyay and R. Mandal, Vacuum stability in an extended standard model with a leptoquark, Phys. Rev. D **95**, 035007 (2017).

[38] S. Sahoo, R. Mohanta, and A. K. Giri, Explaining the R_K and $R_{D^{(*)}}$ anomalies with vector leptoquarks, Phys. Rev. D **95**, 035027 (2017).

[39] D. A. Faroughy, A. Greljo, and J. F. Kamenik, Confronting lepton flavor universality violation in B decays with high-p_T tau lepton searches at LHC, Phys. Lett. B **764**, 126 (2017).

[40] G. Hiller, D. Loose, and K. Schönwald, Leptoquark flavor patterns & B decay anomalies, J. High Energy Phys. 12 (2016) 027.

[41] B. Bhattacharya, A. Datta, J.-P. Guévin, D. London, and R. Watanabe, Simultaneous explanation of the R_K and $R_{D^{(*)}}$ puzzles: A model analysis, J. High Energy Phys. 01 (2017) 015.

[42] M. Duraisamy, S. Sahoo, and R. Mohanta, Rare semileptonic $B \to K(\pi) l_i^- l_j^+$ decay in a vector leptoquark model, Phys. Rev. D **95**, 035022 (2017).

[43] D. Das, K. Ghosh, M. Mitra, and S. Mondal, Probing sterile neutrinos in the framework of inverse seesaw mechanism through leptoquark productions, Phys. Rev. D **97**, 015024 (2018).

[44] N. Assad, B. Fornal, and B. Grinstein, Baryon number and lepton universality violation in leptoquark and diquark models, Phys. Lett. **B777**, 324 (2018).

[45] U. K. Dey, D. Kar, M. Mitra, M. Spannowsky, and A. C. Vincent, Searching for leptoquarks at IceCube and the LHC, Phys. Rev. D **98**, 035014 (2018).

[46] A. Biswas, D. K. Ghosh, S. K. Patra, and A. Shaw, $b \to c\ell\nu$ anomalies in light of extended scalar sectors, Int. J. Mod. Phys. A **34**, 1950112 (2019).

[47] P. Bandyopadhyay and R. Mandal, Revisiting scalar leptoquark at the LHC, Eur. Phys. J. C **78**, 491 (2018).

[48] U. Aydemir, D. Minic, C. Sun, and T. Takeuchi, B-decay anomalies and scalar leptoquarks in unified Pati-Salam models from noncommutative geometry, J. High Energy Phys. 09 (2018) 117.

[49] S. Sahoo and R. Mohanta, Impact of vector leptoquark on $\bar{B} \to \bar{K}^* l^+ l^-$ anomalies, J. Phys. G **45**, 085003 (2018).

[50] J. Kumar, D. London, and R. Watanabe, Combined explanations of the $b \to s\mu^+\mu^-$ and $b \to c\tau^-\bar{\nu}$ anomalies: A general model analysis, Phys. Rev. D **99**, 015007 (2019).

[51] A. Crivellin, C. Greub, D. Müller, and F. Saturnino, Importance of Loop Effects in Explaining the Accumulated Evidence for New Physics in B Decays with a Vector Leptoquark, Phys. Rev. Lett. **122**, 011805 (2019).

[52] S. Mandal, M. Mitra, and N. Sinha, Probing leptoquarks and heavy neutrinos at the LHeC, Phys. Rev. D **98**, 095004 (2018).

[53] A. Biswas, D. K. Ghosh, N. Ghosh, A. Shaw, and A. K. Swain, Collider signature of U_1 Leptoquark and constraints from $b \to c$ observables, J. Phys. G **47**, 045005 (2020).

[54] R. Mandal, Fermionic dark matter in leptoquark portal, Eur. Phys. J. C **78**, 726 (2018).

[55] A. Angelescu, D. Bečirević, D. Faroughy, and O. Sumensari, Closing the window on single leptoquark solutions to the B-physics anomalies, J. High Energy Phys. 10 (2018) 183.

[56] S. Balaji, R. Foot, and M. A. Schmidt, Chiral SU(4) explanation of the $b \to s$ anomalies, Phys. Rev. D **99**, 015029 (2019).

[57] T. Mandal, S. Mitra, and S. Raz, $R_{D^{(*)}}$ motivated $\mathcal{S}_1$ leptoquark scenarios: Impact of interference on the exclusion limits from LHC data, Phys. Rev. D **99**, 055028 (2019).

[58] E. Alvarez and M. Szewc, Nonresonant leptoquark with multigeneration couplings for $\mu\mu jj$ and $\mu\nu jj$ at the LHC, Phys. Rev. D **99**, 095004 (2019).

[59] A. Biswas, A. Shaw, and A. K. Swain, Collider signature of V_2 Leptoquark with $b \to s$ flavour observables, Lett. High Energy Phys. **2**, 126 (2019).

[60] S. Iguro, T. Kitahara, Y. Omura, R. Watanabe, and K. Yamamoto, D* polarization vs. $R_{D^{(*)}}$ anomalies in the leptoquark models, J. High Energy Phys. 02 (2019) 194.

[61] J. Aebischer, A. Crivellin, and C. Greub, QCD improved matching for semileptonic B decays with leptoquarks, Phys. Rev. D **99**, 055002 (2019).

[62] J. Roy, Probing leptoquark chirality via top polarization at the Colliders, arXiv:1811.12058.

[63] B. Fornal, S. A. Gadam, and B. Grinstein, Left-right SU(4) vector leptoquark model for flavor anomalies, Phys. Rev. D **99**, 055025 (2019).

[64] S. Bar-Shalom, J. Cohen, A. Soni, and J. Wudka, Phenomenology of TeV-scale scalar leptoquarks in the EFT, Phys. Rev. D **100**, 055020 (2019).

[65] T. J. Kim, P. Ko, J. Li, J. Park, and P. Wu, Correlation between $R_{D^{(*)}}$ and top quark FCNC decays in leptoquark models, J. High Energy Phys. 07 (2019) 025.

[66] A. Alves, O. J. P. Éboli, G. Grilli Di Cortona, and R. R. Moreira, Indirect and monojet constraints on scalar leptoquarks, Phys. Rev. D **99**, 095005 (2019).

[67] M. J. Baker, J. Fuentes-Martin, G. Isidori, and M. König, High-p_T signatures in vector–leptoquark models, Eur. Phys. J. C **79**, 334 (2019).

[68] U. Aydemir, T. Mandal, and S. Mitra, Addressing the $\mathbf{R}_{D^{(*)}}$ anomalies with an $\mathbf{S}_1$ leptoquark from $\mathbf{SO(10)}$ grand unification, Phys. Rev. D **101**, 015011 (2020).

[69] C. Cornella, J. Fuentes-Martin, and G. Isidori, Revisiting the vector leptoquark explanation of the B-physics anomalies, J. High Energy Phys. 07 (2019) 168.

[70] J. Zhang, C.-X. Yue, C.-H. Li, and S. Yang, Constraints on scalar and vector leptoquarks from the LHC Higgs data, arXiv:1905.04074.

[71] R. Mandal and A. Pich, Constraints on scalar leptoquarks from lepton and kaon physics, J. High Energy Phys. 12 (2019) 089.

[72] W.-S. Hou, T. Modak, and G.-G. Wong, Scalar leptoquark effects on $B \to \mu\bar{\nu}$ decay, Eur. Phys. J. C **79**, 964 (2019).

[73] R. Coy, M. Frigerio, F. Mescia, and O. Sumensari, New physics in $b \to s\ell\ell$ transitions at one loop, Eur. Phys. J. C **80**, 52 (2020).

[74] B. Allanach, T. Corbett, and M. Madigan, Sensitivity of future Hadron colliders to leptoquark pair production in the Di-Muon Di-Jets channel, Eur. Phys. J. C **80**, 170 (2020).

[75] R. Padhan, S. Mandal, M. Mitra, and N. Sinha, Signatures of $\tilde{R}_2$ class of Leptoquarks at the upcoming ep colliders, Phys. Rev. D **101**, 075037 (2020).

[76] A. Bhaskar, D. Das, B. De, and S. Mitra, Enhancement of Higgs production through leptoquarks at the LHC, arXiv:2002.12571.

[77] P. Bandyopadhyay, S. Dutta, and A. Karan, Investigating the production of leptoquarks by means of zeros of amplitude at photon electron collider, arXiv:2003.11751.

[78] J. C. Pati and A. Salam, Lepton number as the fourth color, Phys. Rev. D **10**, 275 (1974); Phys. Rev. D **11**, 703(E) (1975).

[79] H. Georgi and S. L. Glashow, Unity of All Elementary Particle Forces, Phys. Rev. Lett. **32**, 438 (1974).

[80] B. Schrempp and F. Schrempp, Light leptoquarks, Phys. Lett. **153B**, 101 (1985).

[81] R. Barbier *et al.*, R-parity violating supersymmetry, Phys. Rep. **420**, 1 (2005).

[82] M. Kohda, H. Sugiyama, and K. Tsumura, Lepton number violation at the LHC with leptoquark and diquark, Phys. Lett. B **718**, 1436 (2013).

[83] M. Aaboud *et al.* (ATLAS Collaboration), Searches for scalar leptoquarks and differential cross-section measurements in dilepton-dijet events in proton-proton collisions at a centre-of-mass energy of $\sqrt{s} = 13$ TeV with the ATLAS experiment, Eur. Phys. J. C **79**, 733 (2019).

[84] M. Aaboud *et al.* (ATLAS Collaboration), Searches for third-generation scalar leptoquarks in $\sqrt{s} = 13$ TeV pp collisions with the ATLAS detector, J. High Energy Phys. 06 (2019) 144.

[85] A. M. Sirunyan *et al.* (CMS Collaboration), Search for third-generation scalar leptoquarks decaying to a top quark and a τ lepton at $\sqrt{s} = 13$ TeV, Eur. Phys. J. C **78**, 707 (2018).

[86] A. M. Sirunyan *et al.* (CMS Collaboration), Constraints on models of scalar and vector leptoquarks decaying to a quark and a neutrino at $\sqrt{s} = 13$ TeV, Phys. Rev. D **98**, 032005 (2018).

[87] A. M. Sirunyan *et al.* (CMS Collaboration), Search for Leptoquarks Coupled to Third-Generation Quarks in Proton-Proton Collisions at $\sqrt{s} = 13$ TeV, Phys. Rev. Lett. **121**, 241802 (2018).

[88] CMS Collaboration, Projection of searches for pair production of scalar leptoquarks decaying to a top quark and a charged lepton at the HL-LHC, CERN Tech. Report No. CMS-PAS-FTR-18-008, 2018.

[89] K. Chandak, T. Mandal, and S. Mitra, Hunting for scalar leptoquarks with boosted tops and light leptons, Phys. Rev. D **100**, 075019 (2019).

[90] N. Vignaroli, Seeking leptoquarks in the $\mathbf{t\bar{t}}$ plus missing energy channel at the high-luminosity LHC, Phys. Rev. D **99**, 035021 (2019).

[91] W. Buchmuller, R. Ruckl, and D. Wyler, Leptoquarks in lepton—quark collisions, Phys. Lett. B **191**, 442 (1987); Phys. Lett. B **448**, 320(E) (1999).

[92] J. Blumlein, E. Boos, and A. Pukhov, Leptoquark pair production at ep colliders, Mod. Phys. Lett. A **09**, 3007 (1994).

[93] J. Blumlein, E. Boos, and A. Kryukov, Leptoquark pair production in hadronic interactions, Z. Phys. C **76**, 137 (1997).

[94] I. Doršner, S. Fajfer, A. Greljo, J. F. Kamenik, and N. Košnik, Physics of leptoquarks in precision experiments and at particle colliders, Phys. Rep. **641**, 1 (2016).

[95] J. E. Camargo-Molina, A. Celis, and D. A. Faroughy, Anomalies in Bottom from new physics in top, Phys. Lett. B **784**, 284 (2018).

[96] T. Mandal and S. Mitra, Probing color octet electrons at the LHC, Phys. Rev. D **87**, 095008 (2013).

[97] T. Mandal, S. Mitra, and S. Seth, Single productions of colored particles at the LHC: An example with scalar leptoquarks, J. High Energy Phys. 07 (2015) 028.

[98] T. Mandal, S. Mitra, and S. Seth, Probing compositeness with the CMS $eejj$ & eej data, Phys. Lett. B **758**, 219 (2016).

[99] A. Alloul, N. D. Christensen, C. Degrande, C. Duhr, and B. Fuks, FeynRules 2.0–A complete toolbox for tree-level phenomenology, Comput. Phys. Commun. **185**, 2250 (2014).

[100] C. Degrande, C. Duhr, B. Fuks, D. Grellscheid, O. Mattelaer, and T. Reiter, UFO–The Universal FeynRules output, Comput. Phys. Commun. **183**, 1201 (2012).

[101] J. Alwall, R. Frederix, S. Frixione, V. Hirschi, F. Maltoni, O. Mattelaer, H.-S. Shao, T. Stelzer, P. Torrielli, and M. Zaro, The automated computation of tree-level and next-to-leading order differential cross sections, and their matching to parton shower simulations, J. High Energy Phys. 07 (2014) 079.

[102] R. D. Ball *et al.*, Parton distributions with LHC data, Nucl. Phys. **B867**, 244 (2013).

[103] T. Sjostrand, S. Mrenna, and P. Z. Skands, PYTHIA 6.4 physics and manual, J. High Energy Phys. 05 (2006) 026.

[104] J. de Favereau, C. Delaere, P. Demin, A. Giammanco, V. Lemaître, A. Mertens, and M. Selvaggi (DELPHES 3 Collaboration), DELPHES 3, A modular framework for fast simulation of a generic collider experiment, J. High Energy Phys. 02 (2014) 057.

[105] Y. L. Dokshitzer, G. D. Leder, S. Moretti, and B. R. Webber, Better jet clustering algorithms, J. High Energy Phys. 08 (1997) 001.

[106] M. Cacciari, G. P. Salam, and G. Soyez, FastJet user manual, Eur. Phys. J. C **72**, 1896 (2012).

[107] T. Plehn, M. Spannowsky, M. Takeuchi, and D. Zerwas, Stop reconstruction with tagged tops, J. High Energy Phys. 10 (2010) 078.

[108] B. Diaz, M. Schmaltz, and Y.-M. Zhong, The leptoquark Hunter's guide: Pair production, J. High Energy Phys. 10 (2017) 097.

[109] A. Bhaskar, T. Mandal, S. Mitra, and C. Neeraj (to be published).

[110] S. Catani, L. Cieri, G. Ferrera, D. de Florian, and M. Grazzini, Vector Boson Production at Hadron Colliders: A Fully Exclusive QCD Calculation at NNLO, Phys. Rev. Lett. **103**, 082001 (2009).

[111] G. Balossini, G. Montagna, C. M. Carloni Calame, M. Moretti, O. Nicrosini, F. Piccinini, M. Treccani, and A. Vicini, Combination of electroweak and QCD corrections to single W production at the Fermilab Tevatron and the CERN LHC, J. High Energy Phys. 01 (2010) 013.

[112] J. M. Campbell, R. K. Ellis, and C. Williams, Vector boson pair production at the LHC, J. High Energy Phys. 07 (2011) 018.

[113] N. Kidonakis, Theoretical results for electroweak-boson and single-top production, Proc. Sci., DIS2015 (**2015**) 170, [arXiv:1506.04072].

[114] C. Muselli, M. Bonvini, S. Forte, S. Marzani, and G. Ridolfi, Top quark pair production beyond NNLO, J. High Energy Phys. 08 (2015) 076.

[115] A. Kulesza, L. Motyka, D. Schwartländer, T. Stebel, and V. Theeuwes, Associated production of a top quark pair with a heavy electroweak gauge boson at NLO + NNLL accuracy, Eur. Phys. J. C **79**, 249 (2019).